CLEO CONF 96-15
ICHEP96 PA01-085

First Observation of $\tau \to 3h\eta\nu_\tau$ and $\tau \to f_1\pi\nu_\tau$

(CLEO Collaboration)

(July 20, 1996)

Abstract

We have observed a new channel for tau decays with a neutrino, 3 charged hadrons and η in the final state. An observation is made in 3-prong tau decays where the η is reconstructed from its $\eta \to \gamma\gamma$ and $\eta \to 3\pi^\circ$ decays. The measured branching fraction $\mathcal{B}(\tau^- \to h^-h^+h^-\eta\nu_\tau) = (4.1 \pm 0.7 \pm 0.7) \cdot 10^{-4}$ is about two orders of magnitude larger than the theoretical prediction. The hadronic final state exhibits a substructure with clear evidence of significant $f_1(1285)$ production. We also observe the decay $\tau^- \to f_1\pi^-\nu_\tau$ in the $f_1 \to \eta\pi^\circ\pi^\circ$ decay channel. The combined branching fraction is $\mathcal{B}(\tau^- \to f_1\pi^-\nu_\tau) = (6.7 \pm 1.4 \pm 2.2) \cdot 10^{-4}$. Corroborating signals for $f_1(1285)$ production are found also in 5-prong tau decays.

T. E. Coan,[1] V. Fadeyev,[1] I. Korolkov,[1] Y. Maravin,[1] I. Narsky,[1] V. Shelkov,[1] R. Stroynowski,[1] J. Staeck,[1] I. Volobouev,[1] J. Ye,[1] M. Artuso,[2] A. Efimov,[2] M. Gao,[2] M. Goldberg,[2] R. Greene,[2] F. Frasconi,[2] D. He,[2] S. Kopp,[2] G. C. Moneti,[2] R. Mountain,[2] Y. Mukhin,[2] S. Schuh,[2] T. Skwarnicki,[2] S. Stone,[2] X. Xing,[2] J. Bartelt,[3] S. E. Csorna,[3] V. Jain,[3] S. Marka,[3] A. Freyberger,[4] R. Godang,[4] D. Gibaut,[4] K. Kinoshita,[4] I. C. Lai,[4] P. Pomianowski,[4] S. Schrenk,[4] G. Bonvicini,[5] D. Cinabro,[5] L. Perera,[5] B. Barish,[6] M. Chadha,[6] S. Chan,[6] G. Eigen,[6] J. S. Miller,[6] C. O'Grady,[6] M. Schmidtler,[6] J. Urheim,[6] A. J. Weinstein,[6] F. Würthwein,[6] D. M. Asner,[7] D. W. Bliss,[7] W. S. Brower,[7] G. Masek,[7] H. P. Paar,[7] J. Gronberg,[8] C. M. Korte,[8] D. J. Lange,[8] R. Kutschke,[8] S. Menary,[8] R. J. Morrison,[8] S. Nakanishi,[8] H. N. Nelson,[8] T. K. Nelson,[8] C. Qiao,[8] J. D. Richman,[8] D. Roberts,[8] A. Ryd,[8] H. Tajima,[8] M. S. Witherell,[8] R. Balest,[9] B. H. Behrens,[9] K. Cho,[9] W. T. Ford,[9] H. Park,[9] P. Rankin,[9] J. Roy,[9] J. G. Smith,[9] J. P. Alexander,[10] C. Bebek,[10] B. E. Berger,[10] K. Berkelman,[10] K. Bloom,[10] D. G. Cassel,[10] H. A. Cho,[10] D. M. Coffman,[10] D. S. Crowcroft,[10] M. Dickson,[10] P. S. Drell,[10] R. Ehrlich,[10] R. Elia,[10] A. D. Foland,[10] P. Gaidarev,[10] R. S. Galik,[10] B. Gittelman,[10] S. W. Gray,[10] D. L. Hartill,[10] B. K. Heltsley,[10] P. I. Hopman,[10] S. L. Jones,[10] J. Kandaswamy,[10] N. Katayama,[10] P. C. Kim,[10] D. L. Kreinick,[10] T. Lee,[10] Y. Liu,[10] G. S. Ludwig,[10] J. Masui,[10] J. Mevissen,[10] N. B. Mistry,[10] C. R. Ng,[10] E. Nordberg,[10] M. Ogg,[10,*] J. R. Patterson,[10] D. Peterson,[10] D. Riley,[10] A. Soffer,[10] C. Ward,[10] P. Avery,[11] M. Athanas,[11] C. D. Jones,[11] M. Lohner,[11] C. Prescott,[11] S. Yang,[11] J. Yelton,[11] J. Zheng,[11] G. Brandenburg,[12] R. A. Briere,[12] D. Y.-J. Kim,[12] T. Liu,[12] M. Saulnier,[12] R. Wilson,[12] H. Yamamoto,[12] T. E. Browder,[13] F. Li,[13] Y. Li,[13] J. L. Rodriguez,[13] T. Bergfeld,[14] B. I. Eisenstein,[14] J. Ernst,[14] G. E. Gladding,[14] G. D. Gollin,[14] E. Johnson,[14] I. Karliner,[14] M. Palmer,[14] M. Selen,[14] J. J. Thaler,[14] K. W. Edwards,[15] A. Bellerive,[16] D. I. Britton,[16] R. Janicek,[16] D. B. MacFarlane,[16] K. W. McLean,[16] P. M. Patel,[16] A. J. Sadoff,[17] R. Ammar,[18] P. Baringer,[18] A. Bean,[18] D. Besson,[18] D. Coppage,[18] C. Darling,[18] R. Davis,[18] N. Hancock,[18] S. Kotov,[18] I. Kravchenko,[18] N. Kwak,[18] S. Anderson,[19] Y. Kubota,[19] M. Lattery,[19] J. J. O'Neill,[19] S. Patton,[19] R. Poling,[19] T. Riehle,[19] A. Smith,[19] V. Savinov,[19] M. S. Alam,[20] S. B. Athar,[20] Z. Ling,[20] A. H. Mahmood,[20] H. Severini,[20] S. Timm,[20] F. Wappler,[20] A. Anastassov,[21] S. Blinov,[21,†] J. E. Duboscq,[21] R. Fulton,[21] D. Fujino,[21] K. K. Gan,[21] T. Hart,[21] K. Honscheid,[21] H. Kagan,[21] R. Kass,[21] J. Lee,[21] M. Sung,[21] A. Undrus,[21,†] R. Wanke,[21] A. Wolf,[21] M. M. Zoeller,[21] B. Nemati,[22] S. J. Richichi,[22] W. R. Ross,[22] P. Skubic,[22] M. Wood,[22] M. Bishai,[23] J. Fast,[23] E. Gerndt,[23] J. W. Hinson,[23] D. H. Miller,[23] E. I. Shibata,[23] I. P. J. Shipsey,[23] M. Yurko,[23] L. Gibbons,[24] S. D. Johnson,[24] Y. Kwon,[24] S. Roberts,[24] E. H. Thorndike,[24] C. P. Jessop,[25] K. Lingel,[25] H. Marsiske,[25] M. L. Perl,[25] S. F. Schaffner,[25] D. Ugolini,[25] R. Wang,[25] and X. Zhou[25]

[1]Southern Methodist University, Dallas, Texas 75275
[2]Syracuse University, Syracuse, New York 13244
[3]Vanderbilt University, Nashville, Tennessee 37235

[*]Permanent address: University of Texas at Austin.

[†]Permanent address: BINP, RU-630090 Novosibirsk, Russia.

[4]Virginia Polytechnic Institute and State University, Blacksburg, Virginia 24061
[5]Wayne State University, Detroit, Michigan 48202
[6]California Institute of Technology, Pasadena, California 91125
[7]University of California, San Diego, La Jolla, California 92093
[8]University of California, Santa Barbara, California 93106
[9]University of Colorado, Boulder, Colorado 80309-0390
[10]Cornell University, Ithaca, New York 14853
[11]University of Florida, Gainesville, Florida 32611
[12]Harvard University, Cambridge, Massachusetts 02138
[13]University of Hawaii at Manoa, Honolulu, Hawaii 96822
[14]University of Illinois, Champaign-Urbana, Illinois 61801
[15]Carleton University, Ottawa, Ontario, Canada K1S 5B6
and the Institute of Particle Physics, Canada
[16]McGill University, Montréal, Québec, Canada H3A 2T8
and the Institute of Particle Physics, Canada
[17]Ithaca College, Ithaca, New York 14850
[18]University of Kansas, Lawrence, Kansas 66045
[19]University of Minnesota, Minneapolis, Minnesota 55455
[20]State University of New York at Albany, Albany, New York 12222
[21]Ohio State University, Columbus, Ohio 43210
[22]University of Oklahoma, Norman, Oklahoma 73019
[23]Purdue University, West Lafayette, Indiana 47907
[24]University of Rochester, Rochester, New York 14627
[25]Stanford Linear Accelerator Center, Stanford University, Stanford, California 94309

Tau decays with an η meson in the final state provide important information about the behavior and violations of various hadronic symmetries and allow for a study of the resonant structure of the weak hadronic current. These decays are rare and their detection became possible only recently in the high statistics CLEO experiment at CESR. Two such decays with small branching fractions have been observed: $\mathcal{B}(\tau^- \to \pi^-\pi^\circ\eta\nu_\tau) = (0.17 \pm 0.2 \pm 0.2)\%$ [1] and $\mathcal{B}(\tau^- \to K^-\eta\nu_\tau) = (0.026 \pm 0.05 \pm 0.05)\%$ [2]. The former has also been reported by the ALEPH group [3]. All other tau decays involving η mesons were expected to be severely suppressed by the chiral anomaly term and by phase space constraints and to have very small branching fractions. The decay $\tau^- \to h^-h^+h^-\eta\nu_\tau$ can proceed through the axial-vector current, and its branching fraction is predicted to be $1.2 \cdot 10^{-6}$ [4].

In this paper, we present an observation of the tau decay $\tau^- \to h^-h^+h^-\eta\nu_\tau$ [1] with the η reconstructed from the $\gamma\gamma$ and $3\pi^\circ$ decay modes. We make no particle identification of charged tracks but from phase-space arguments and evidence of resonant substructure of the final state it appears that all the charged tracks are pions. Within the limits of our particle identification capabilities, data are consistent with this assumption. We use pion mass assignments throughout the paper.

We use data obtained by the CLEO II detector at the Cornell Electron Storage Ring operating at the center of mass energy corresponding to the peak of the $\Upsilon(4S)$ resonance (10.6 GeV) and 60 MeV below this energy. The data correspond to an integrated luminosity of 4.86 fb^{-1} and contain about 4.27 million $\tau^+\tau^-$ pairs. CLEO II is a general purpose solenoidal spectrometer described in detail in Ref. [5]. In addition to good quality tracking its special feature is a 7800-crystal CsI(Tl) electromagnetic calorimeter allowing for photon detection with high efficiency and good energy and angular resolution essential for η and π^0 reconstruction.

We start by searching for $\eta \to \gamma\gamma$ decays. We select $\tau^- \to h^-h^+h^-\eta\nu_\tau$ events having the 1-vs-3 prong event topology, where one of the taus decays into a single prong: electron, muon or hadron. The second tau – representing the signal candidate – should have three charged tracks and at least two well identified photons among its decay products. Candidate eta-decay photons are identified as isolated clusters with energies greater than 200 MeV in the calorimeter and photon-like lateral energy profile. The more energetic candidate photon is required to be above 400 MeV. Both photons are required to be in the barrel part of the calorimeter ($|\cos\theta_\gamma| < 0.8$) and make only one pair combination that satisfies the requirement that $-12.0 < S_{\gamma\gamma} = (m_{\gamma\gamma} - m_\eta)/\sigma_{\gamma\gamma} < 10.5$, where $\sigma_{\gamma\gamma}$ is the η mass resolution calculated by propagating angular and energy resolution of each of the two photons and is typically 10 MeV.

We require an electron candidate to have momentum, p, above 0.5 GeV/c and energy deposition in the calorimeter, E, such that $0.9 < E/p < 1.1$. If specific ionization information is available, we veto the event if it is more than 2 standard deviations below the expected value. We require a muon candidate to penetrate at least 3 absorption lengths of iron for track momenta smaller than 2.0 GeV/c, and more than 5 absorption lengths for momenta above 2.0 GeV/c. For electron- and muon-tagged events no photons are allowed in the tag

[1] Throughout this paper charge conjugation is implied. Here, h stands for either π or K.

hemisphere with energy above 75 MeV. A hadron tag is a track which is identified neither as an electron nor as a muon and has an invariant mass with all photon candidates in the tag hemisphere smaller than 0.5 GeV/c^2. In addition to single pions, this tag recovers unidentified electrons and muons and a small fraction of $\tau^- \to \rho^- \nu_\tau$ decays.

There are several sources of background simulating the tau-pair 1-vs-3 topology. Among those, the dominant sources are: low multiplicity $q\bar{q}$ production, 2-photon processes, feed-across from other tau decays and radiative-Bhabha and muon pair production. They contribute in different proportions to different tags.

To suppress $e^+e^- \to e^+e^-(\gamma)$ and $e^+e^- \to \mu^+\mu^-(\gamma)$ events with subsequent $\gamma \to e^+e^-$ conversion, we do not allow any track to have more than 85% of the beam energy. To remove background due to 2-photon processes, we restrict the total transverse momentum in the event to be greater than 0.3 GeV/c and require the direction of the missing momentum in the event to satisfy $|\cos\theta_{miss}| < 0.95$. The contribution from low multiplicity $q\bar{q}$ events and incompletely reconstructed tau events is minimized by rejecting events with additional photons in the 3-prong hemisphere with energies above 120 MeV. For the hadron-tag we reduce $q\bar{q}$ and 2-photon backgrounds by vetoing the event if the missing mass is less then $0.1E_{cm}$ or greater than $0.5E_{cm}$. In addition hadron tag candidates are rejected if the angle between the tag track and the beam satisfies $|\cos\theta| > 0.81$.

Further suppression of random-photon background in the hadron tag sample is obtained by more restrictive criteria on the energy of the photon candidates. We require the less energetic of the two photons in the signal hemisphere to be above 250 MeV and the more energetic photon to be above 700 MeV. We also remove events containing $K_s^0 \to \pi^+\pi^-$ decays in the signal hemisphere.

To search for the existence of η mesons we calculate the invariant mass of the two photons, shown in Fig. 1, and find an enhancement at the η mass. The normalized mass $S_{\gamma\gamma}$, shown in Fig. 2, is a better variable since it accounts for the energy dependence of the 2γ mass resolution, $\sigma_{\gamma\gamma}$.

Also plotted is random-pair background estimated from the KORALB generator for tau-pair production in e^+e^- annihilations, combined with the TAUOLA decay package [6], where taus are allowed to decay into all known final states [7], and a GEANT-based [8] detector simulation. Based on the Monte Carlo studies of the η shape we define an η signal region to be $-3 < S_{\gamma\gamma} < 2$. This region contains 106 events. The random pair background can be removed either by fitting the $S_{\gamma\gamma}$ distribution or by performing sideband subtractions. We use fitting to extract the final $\tau^- \to h^-h^+h^-\eta\nu_\tau$ signal and use sideband subtraction to determine $q\bar{q}$ background and resonant substructure.

We define $S_{\gamma\gamma}$ sidebands as $-9 < S_{\gamma\gamma} < -4$ and $3 < S_{\gamma\gamma} < 8$. Monte Carlo studies of the background show it to be a nearly linear function of $S_{\gamma\gamma}$ and the systematic error associated with the sideband subtraction procedure is very small. Since sideband subtraction does not remove events which contain real η mesons, background remains from the $\tau^- \to \eta\pi^-\pi^\circ\nu_\tau$ channel, estimated to be 1.0 ± 0.3 events.

We use independent data samples to estimate background due to $e^+e^- \to q\bar{q}$ events and 2-photon interactions. We select $q\bar{q}$ events by requiring the invariant mass of the charged track and photons in the tag hemisphere to be more than the mass of the τ. On the signal side we keep the same cuts as described above except for the minimal energy cut for the η photon candidates. This cut is relaxed to 200 MeV for both photons. We then follow the

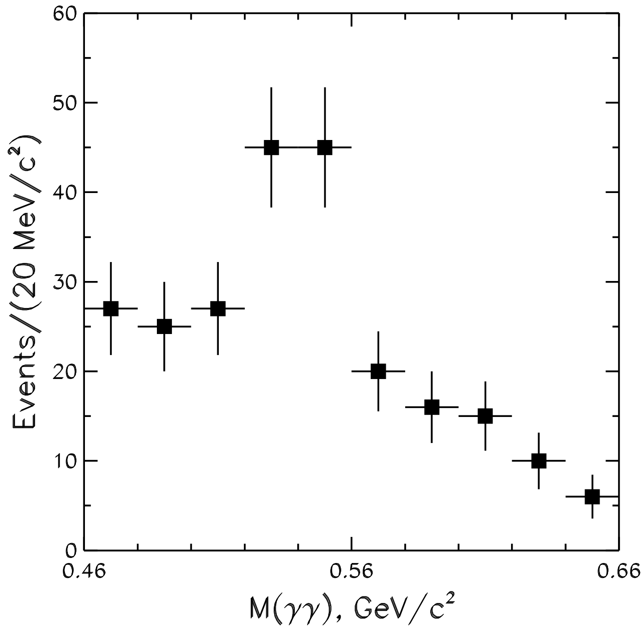

FIG. 1. Two-photon invariant mass distribution for data events.

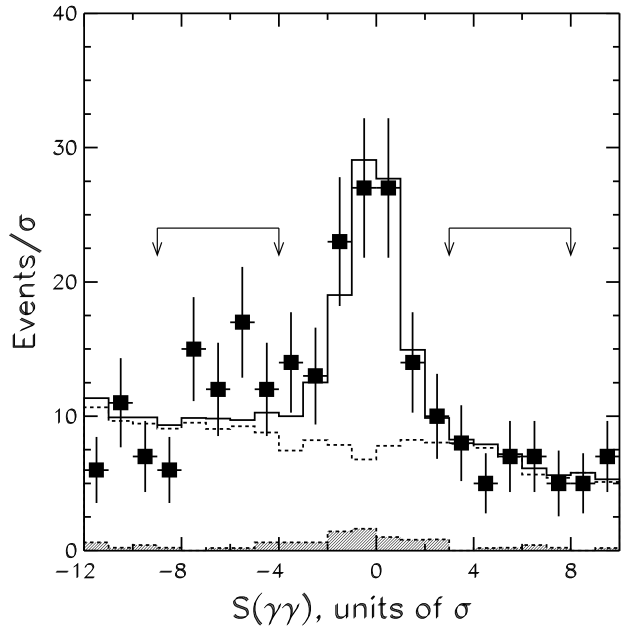

FIG. 2. $S_{\gamma\gamma} = (m_{\gamma\gamma} - m_\eta)/\sigma_{\gamma\gamma}$. Solid line describes the fit which includes the η signal (including real background η's) and random-photon background (dashed line). The estimated amount of $q\bar{q}$ background is shown by the hatched area. Arrows indicate the range used for sideband subtraction.

same η identification procedure as for the signal events. This sample provides the shape of the $q\bar{q}$ background. The normalization is obtained from a fit to the data above 1.8 GeV/c^2 in the distribution of the $3\pi\eta$ invariant mass and is illustrated in Fig. 3 as a shaded area. We estimate that in the region below the τ mass there is a background of 5.0 ± 1.5 $q\bar{q}$ events contributing to the $3h\eta$ signal. From studies of 2-photon interaction data, we conservatively estimate that less than 1.0 events from such processes survive all selection criteria. The hadronic mass distribution of the selected events, plotted in Fig. 3, peaks below the τ mass and is much larger than the extrapolated $q\bar{q}$ background.

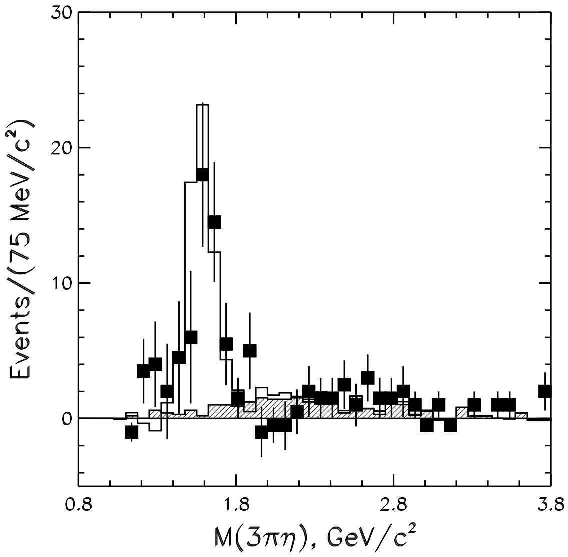

FIG. 3. Invariant mass $M_{3\pi\eta}$ after $S_{\gamma\gamma}$ sideband subtraction. Shaded area describes $q\bar{q}$ background. Solid line represents the fit described in the text.

The number of signal events is obtained from a fit to the $S_{\gamma\gamma}$ distribution for events with $3\pi\eta$ mass smaller then m_τ. The fit is illustrated in Fig. 2. The fit includes the expected shape of the η signal determined from the $\tau^- \to \pi^-\pi^+\pi^-\eta\nu_\tau$ Monte Carlo simulation and the shape of the random-pair background (dashed line). The fit yield of 65.1 ± 12.9 events includes the small tau feed-across and $q\bar{q}$ backgrounds discussed above. The $S_{\gamma\gamma}$ distribution from the $q\bar{q}$ background sample is shown for illustration only as the hatched area in Fig. 2. As a cross check, the fit is performed separately for leptonic and hadronic tags and in each case the η signal is clearly observed and the corresponding signal sizes are consistent with expectations from the combined sample. The results are listed in Table I together with event selection efficiencies (ε), estimated $q\bar{q}$ background ($N_{q\bar{q}}$) and calculated branching fractions.

The overall systematic error is estimated to be 21%. This error is due to the following uncertainties: estimate of the number of tau pairs (1.4%), acceptance and reconstruction efficiency (7.0%), background shape (15%), background normalization (2%) and uncertainty of the choice of spectral functions used in Monte Carlo simulations (13%) (see below). Systematic errors associated with the Monte Carlo were obtained by repeating the efficiency calculations assuming different decay chains. Thus, the final branching fraction for the $\eta \to \gamma\gamma$ mode is

$$\mathcal{B}(\tau^- \to h^-h^+h^-\eta\nu_\tau) = (3.8 \pm 0.8 \pm 0.8) \cdot 10^{-4}.$$

TABLE I. The number of signal and background events, efficiencies and branching fractions for the $\tau \to 3h\eta\nu_\tau$ and $\tau \to f_1\pi\nu_\tau$ decays obtained from fits to separate and combined data samples.

Channel	Tag	Events	$N_{q\bar{q}}$	$\varepsilon_e[\%]$	$\varepsilon_\mu[\%]$	$\varepsilon_\pi[\%]$	$\varepsilon_\rho[\%]$	$\mathcal{B}(\times 10^{-4})$
$3h\eta\nu_\tau$	e	31.6±8.2	0.0±0.9	9.4				5.7±1.5
	μ	9.8±6.3	0.1±0.9		9.0	0.2		1.9±1.2
	h	23.9±7.0	5.0±1.1	1.4	2.3	6.3	0.8	3.7±1.4
	e,μ,h	65.1±12.9	5.0±1.5	10.8	11.3	6.3	0.8	3.8±0.8
$f_1\pi\nu_\tau$	e,μ,h	30.4±8.8	-	9.3	9.8	5.8	0.8	6.0±1.7

Tau decays to an η and pions in the final state can proceed through a number of different resonances. Possible intermediate states will affect the signal efficiency calculation. We plot the invariant mass distribution of $\eta\pi^+\pi^-$ (2 entries/event) in Fig. 4a using the mass-constrained η momentum and assuming pion mass assignment for the charged tracks. The most prominent peak corresponds to $f_1(1285)$ production. In Fig. 4b we show the plot of the $\eta\pi^+\pi^-$ mass vs the $\eta\pi$ mass, with 4 entries per event. It shows higher population density in the $f_1(1285)$ vs $a_0(980)$ region, suggesting the presence of an expected $a_0(980)$ intermediate state. The apparent shift of the $\eta\pi$ mass from the a_0 peak is partly due to the high proportion of wrong $\eta\pi$ mass combinations in this plot.

For the signal Monte Carlo we use the axial-vector decay chain $\tau \to f_1(1285)\pi\nu_\tau$ with $f_1(1285) \to a_0^+(980)\pi^-$ and $a_0^+(980) \to \eta\pi^+$. We assume the spectral function shape to be dominated by the $a_1(1260)$, where the $f_1(1285)$ and π are in a P-wave [9].

A fit of the background-subtracted data is shown in Fig. 5. We restrict the fit range to avoid addressing the question whether there is additional structure in Fig. 4a. For the cases where both entries fall within this portion of the $\eta\pi^+\pi^-$ spectrum (74% of the events according to the Monte Carlo simulation), we weight each entry by 0.5. We fit the data to a Monte Carlo f_1 shape which includes both right and wrong $\eta\pi^+\pi^-$ combinations, plus a positive-definite constant background component to account for possible non-$f_1\pi$ signal. The result of the fit is indicated by the solid histogram, while the dotted line shows the fit result for the background term (the fit prefers no non-$f_1\pi$ background). The fit results are given in Table I and correspond to a branching fraction $\mathcal{B}(\tau \to f_1\pi\nu_\tau) = (6.0 \pm 1.7) \cdot 10^{-4}$. This value has been calculated using $\mathcal{B}(f_1(1285) \to \eta\pi\pi) = 0.54 \pm 0.15$ [7] and the isospin prediction that 2/3 of $\eta\pi\pi$ is in the $\eta\pi^+\pi^-$ state. The systematic error for this decay has similar components as for the $3h\eta$ analysis, except for the negligible contribution of the $q\bar{q}$ background, and is equal to 21%. This is dominated by 15% arising from variation of the background shape and fit region. Including an additional uncertainty of 28% associated with the error on the $f_1(1285) \to \eta\pi\pi$ decay rate, we find the measured decay branching fraction from this $\eta \to \gamma\gamma$ analysis to be

$$\mathcal{B}(\tau^- \to f_1\pi^-\nu_\tau) = (6.0 \pm 1.7 \pm 2.1) \cdot 10^{-4}.$$

In Table II we list the expected contributions from $\tau^- \to h^-h^+h^-\eta\nu_\tau$ and $\tau^- \to f_1\pi^-\nu_\tau$ to several other τ final states. Of these, observations in all except the $3\pi^\pm 2\pi^\circ$ final state seem feasible, so we search for such decays in the final states $3\pi^\pm 3\pi^\circ$, $5\pi^\pm\pi^\circ$, $5\pi^\pm$, and $h^\pm\pi^\circ\pi^\circ\eta$.

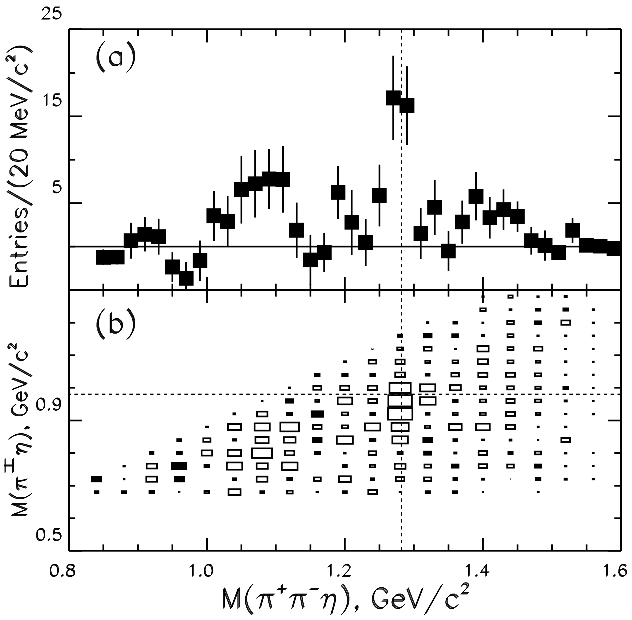

FIG. 4. (a) Mass of the $\eta\pi^+\pi^-$ system after background subtraction, 2 entries/event. (b) Plot of $M_{\pi^+\pi^-\eta}$ vs. $M_{\pi^\pm\eta}$ after sideband subtraction, 4 entries per event. Dotted lines show expected positions of $f_1(1285)$ and $a_0(980)$ resonances. A bin size of 40 MeV is used for both axes.

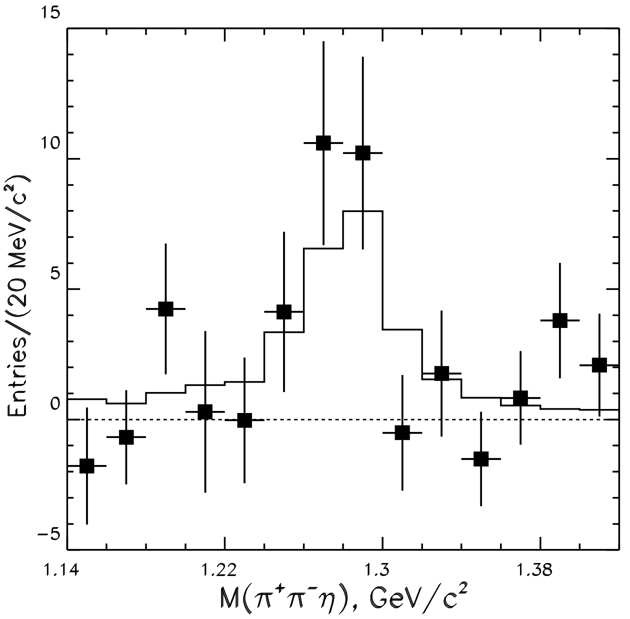

FIG. 5. A fit to the f_1 region of the $\eta\pi^+\pi^-$ mass distribution. The solid histogram describes a fit to the sum of the $f_1(1285)$ signal and the wrong combination $\eta\pi\pi$ background. The dotted line indicates a (null) flat component of the fit which is included to model non-f_1 background in this region.

TABLE II. Expected contributions to various final states in τ decays based on the observation of the $\tau \to 3h\eta\nu_\tau$, $\eta \to \gamma\gamma$ and $\tau \to f_1 h\nu_\tau$ channels, in units of 10^{-4}.

Observed channel	Decay mode	Final state	$\mathcal{B}(\times 10^{-4})$	Comments
$\tau^- \to 3h^-\eta\nu_\tau$	$\eta \to \pi^\circ\pi^\circ\pi^\circ$	$3\pi^\pm 3\pi^\circ$	1.2 ± 0.3	
	$\eta \to \pi^+\pi^-\pi^\circ$	$5\pi^\pm\pi^\circ$	0.9 ± 0.3	$\simeq 50\%$ of $\tau^- \to 5\pi^\pm\pi^\circ\nu_\tau$
$\tau^- \to f_1\pi^-\nu_\tau$	$f_1 \to 2\pi^\pm 2\pi^\pm$	$5\pi^\pm$	0.9 ± 0.5	$\simeq 16\%$ of $\tau^- \to 5\pi^\pm\nu_\tau$
	$f_1 \to 2\pi^\pm 2\pi^\circ$	$3\pi^\pm 2\pi^\circ$	0.9 ± 0.6	$\simeq 2\%$ of $\tau^- \to 3\pi^\pm 2\pi^\circ\nu_\tau$
	$f_1 \to a_0^0(980)\pi^\circ$	$\pi^\pm 2\pi^\circ\eta$	1.1 ± 0.5	

First we search for η production in the decay channel $\tau^- \to \pi^-\pi^+\pi^-3\pi^\circ\nu_\tau$. We apply event selection criteria similar to those described before but limited to leptonic tags only: we select events with 1-vs-3 prong topology, where the 1-prong is identified as an electron or a muon, and require at least six photons in the 3-prong hemisphere. We obtain additional reduction of $q\bar{q}$ background by requiring the magnitude of the total momentum vector of particles in the signal hemisphere to be greater than 65% of the beam energy. The identification of six-photon candidates follows the same requirements as in the previous analysis except for reduction of the minimum required energy deposited in the calorimeter to 30 MeV. To select events with $3\pi^\circ$'s, we apply a global fitting procedure [1], where we require at least one combination of photon pairs in the event to be compatible with the $3\pi^\circ$ hypothesis within the photon pair mass resolution: $\chi^2 < 9$, where

$$\chi^2 = \sum_{i=1}^{3}\left(\frac{M^i_{\gamma\gamma} - M_{\pi^0}}{\sigma^i_{\gamma\gamma}}\right)^2 .$$

In case of more than one possibility we choose the combination with the smallest χ^2. There are 51 events satisfying these criteria, of which 31 events have a 6π mass below the mass of the tau. The invariant mass distribution of the three neutral pions, illustrated in Fig. 6, shows an enhancement at the η mass. Also shown in this figure are the distributions of the $q\bar{q}$ and random-photon background (dashed line) estimated with the same procedure as for the $\eta \to \gamma\gamma$ analysis. The solid line describes the sum of the fit and the background as described below. From the Monte Carlo studies we define a signal region (in units of GeV/c^2) by $0.53 < M(3\pi^\circ) < 0.57$ and sidebands by $0.49 < M(3\pi^\circ) < 0.51$ and $0.59 < M(3\pi^\circ) < 0.61$.

The final η content of 11.2 ± 3.7 events is obtained from a fit to the expected shape of the signal and random-photon background. To study a possible $q\bar{q}$ background contribution to this signal, we plot in Fig. 7 the 6π mass spectrum for data and sideband subtracted $q\bar{q}$ background. The $q\bar{q}$ background appears to be negligible. The efficiency of the event selection procedure is estimated from the Monte Carlo to be $(2.3 \pm 0.1)\%$ and the corresponding branching fraction is

$$\mathcal{B}(\tau^- \to h^-h^+h^-\eta\nu_\tau) = (5.1 \pm 1.7 \pm 1.1) \cdot 10^{-4},$$

in excellent agreement with the measurement from the $\eta \to \gamma\gamma$ channel. Here, the systematic error of 21% has contributions from the uncertainty in the $q\bar{q}$ background estimate (2%), $3\pi^\circ$ reconstruction procedure (9%), χ^2 selection criteria (10%), number of τ pairs produced (2%),

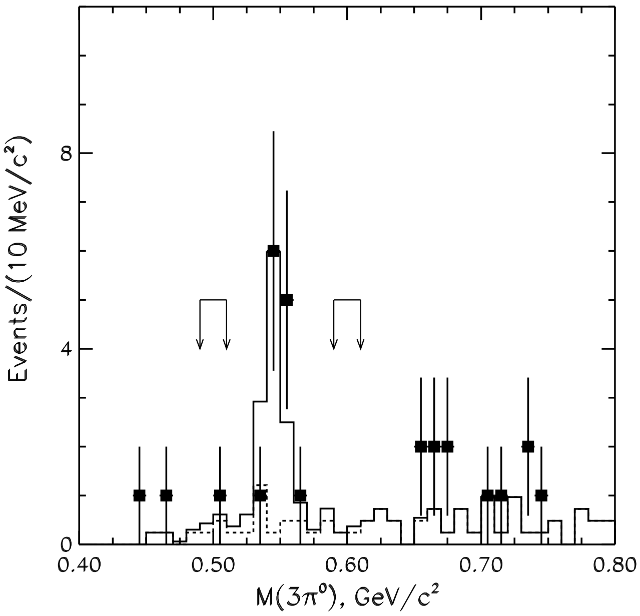

FIG. 6. Mass of the three neutral pions in the $\tau \to 3h3\pi^\circ\nu_\tau$ decay. The solid histogram shows the fit to the Monte Carlo signal shape and random-photon tau background (dashed histogram). Arrows describe the range used for sideband subtraction.

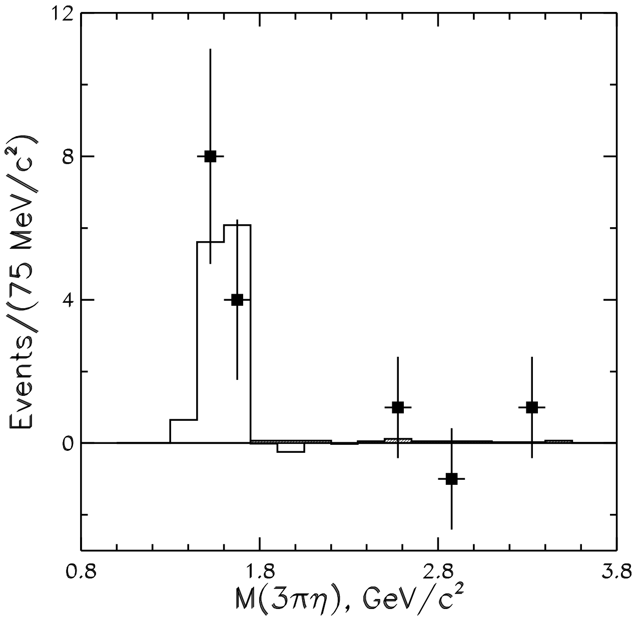

FIG. 7. Sideband-subtracted hadronic mass of the $\tau \to 3h3\pi^\circ\nu_\tau$ decay. Solid line describes the fit that includes the tau background and $q\bar{q}$ background (hatched area).

tracking efficiency (4%), choice of spectral functions (13%), background parameterization (8%), and Monte Carlo statistics (2%),

The results of the measurements of the two η decay modes can be combined to give the decay branching fraction

$$\mathcal{B}(\tau^- \to h^- h^+ h^- \eta\nu_\tau) = (4.1 \pm 0.7 \pm 0.7) \cdot 10^{-4}.$$

The common systematic errors have been separated out in the error propagation procedure.

For 5-prong τ decays we concentrate on the $f_1(1285)$ signal. Again, we apply selection and analysis procedures similar to those described previously. We search for the signal in the 1-vs-5 event topology and use only lepton tags. Background estimates and subtraction also follow a similar procedure. For the $\tau^- \to 3\pi^- 2\pi^+ \pi^\circ \nu_\tau$ channel we reconstruct the neutral pion in the 5-prong hemisphere from photon candidates with energies above 80 MeV. Because we use the leptonic tags only and the random-photon background is much smaller for the π° than for the η, we relax the angular acceptance region for photons forming a π° to $|\cos\theta| < 0.95$. Since there are six possible $\pi^+\pi^-\pi^0$ combinations per event, the η signal is dominated by the combinatorial background. The $2\pi^+ 2\pi^- \pi^\circ$ mass distribution is shown in Fig. 8a. A good description of the data is obtained from a sum of the signal expected from the $f_1 \to \pi^+\pi^-\eta$ contribution (unshaded area) normalized to the branching fraction listed in Table II and the phase-space Monte Carlo expectations (hatched area). Similarly, the $2\pi^+ 2\pi^-$ mass distribution for the decay $\tau^- \to 3\pi^- 2\pi^+ \nu_\tau$, presented in Fig. 8b, cannot be adequately described by a phase-space distribution alone. A better description is obtained after addition of the expected signal from the $f_1 \to 2\pi^+ 2\pi^-$ decay. Fits leaving the relative normalizations of the two components as free parameters yield $\tau \to f_1 \pi \nu_\tau$ branching fractions compatible with previous estimates. For the $5\pi^\pm \pi^\circ$ final state we expect 19.9 ± 6.7 events on the basis of the combined $\tau^- \to h^- h^+ h^- \eta \nu_\tau$ branching fraction and find 26.0 ± 10.4 events and for the $5\pi^\pm$ final state we expect 39.6 ± 24.7 and find 84.6 ± 26.3 events. Since systematic effects associated with the choice of background shapes and resonance content of these τ decays are large and difficult to estimate, we interpret these results only as corroboration of the observed $f_1(1285)$ production in τ decays.

Finally, we present evidence for the decay $\tau \to f_1 \pi \nu_\tau$ through the $\eta\pi^\circ\pi^\circ$ decay mode of the f_1. From isospin, we expect this f_1 decay mode to have a branching fraction one-half as large as the $\eta\pi^+\pi^-$ mode discussed above. We have searched for the final state $h^-\pi^\circ\pi^\circ\eta$ using the $\eta \to \gamma\gamma$ channel, with cuts very similar to those in the $h^- h^+ h^- \eta$ analyses. We choose not to perform sideband subtractions since there are so few events and because of subtleties associated with subtraction in three dimensions (η and two π°'s). In Fig. 9a, we show the $\eta\pi^\circ\pi^\circ$ mass distribution for the 34 events which have a mass of the $h^-\pi^\circ\pi^\circ\eta$ system below the tau mass. For this decay, there is only one $\eta\pi^\circ\pi^\circ$ combination for each event. The solid line represents a fit to a Monte Carlo signal shape plus a linear background. We find a signal of 12.7 ± 4.1 events. Fig. 9b again addresses the issue of whether there is peaking in the region corresponding to the expected $f_1 \to a_0 \pi^\circ$ decay. However in this case, we take advantage of the fact that there are only two $\eta\pi^\circ$ combinations and, due to the kinematics of the $f_1 \to a_0\pi^\circ$ decay, the lower mass combination almost always lies below the actual position of the $a_0(980)$ resonance. Thus we plot only the higher-mass $\eta\pi^\circ$ combination vs the $\eta\pi^\circ\pi^\circ$ mass. The expected enhancement near the $a_0(980)$ mass is evident. While this procedure would distort the shape of the $\eta\pi^\circ$ mass spectrum for $f_1 \to \eta\pi^\circ\pi^\circ$ decays without

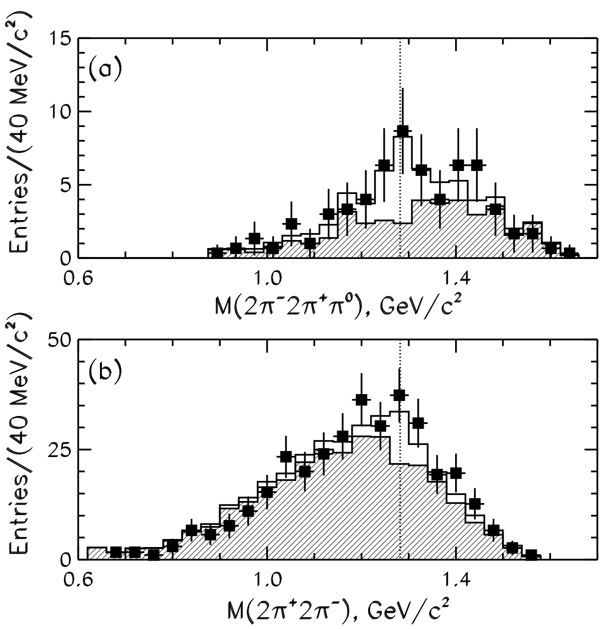

FIG. 8. (a) M($2\pi^+2\pi^-\pi^\circ$), 3 entries/event, for $\tau^- \to 3\pi^-2\pi^+\pi^\circ\nu_\tau$ decays. (b) M($2\pi^+2\pi^-$), 3 entries/event, for $\tau^- \to 3\pi^-2\pi^+\nu_\tau$ decays. Hatched areas correspond to the generic tau Monte Carlo. The solid lines correspond to the fits with normalization of the signal fixed to the measured values. The dotted line marks the position of the $f_1(1285)$ peak.

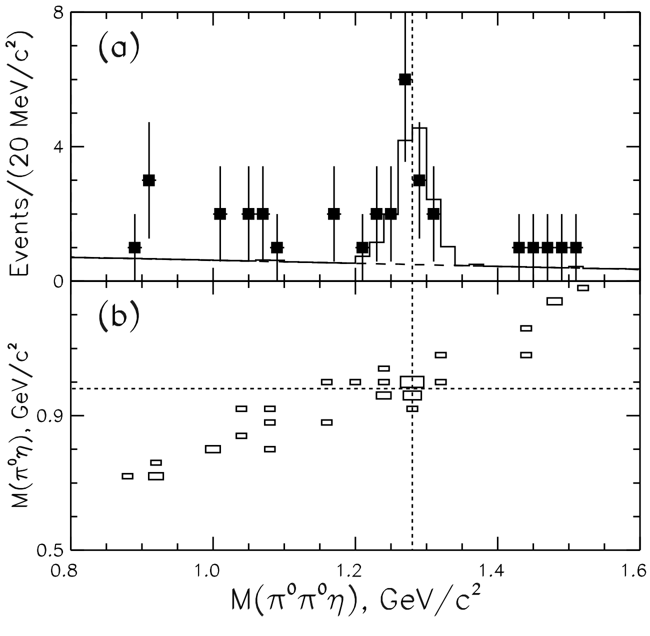

FIG. 9. (a) Mass of the $\eta\pi^\circ\pi^\circ$ system, 1 entry/event. The solid line describes a fit to the sum of a Monte Carlo signal shape plus a linear background function. (b) Plot of $M_{\pi^\circ\pi^\circ\eta}$ vs. the larger of the two $M_{\pi^\circ\eta}$ combinations (see text), 1 entry per event. Dotted lines show expected positions of $f_1(1285)$ and $a_0(980)$ resonances. A bin size of 40 MeV is used for both axes.

an intermediate a_0, we have checked that the procedure does not artificially produce a peak at the $a_0(980)$ mass for such decays.

We use Monte Carlo simulations similar to those used for the $h^-h^+h^-\eta$ analyses to estimate the detection efficiency to be $(3.0 \pm 0.2)\%$. This leads to a branching fraction,

$$\mathcal{B}(\tau \to f_1\pi\nu_\tau) = (8.1 \pm 2.6 \pm 2.6) \cdot 10^{-4}.$$

The systematic errors result predominantly from the fit procedure (8%), absolute π° and η reconstruction efficiency (10%), and uncertainties in the spectral function (10%) and the $f_1 \to \eta\pi\pi$ branching fraction (28%). Since this result is in good agreement with the measurement from the $f_1 \to \eta\pi^+\pi^-$ decay mode we combine the two measurements and find

$$\mathcal{B}(\tau \to f_1\pi\nu_\tau) = (6.7 \pm 1.4 \pm 2.2) \cdot 10^{-4}.$$

The $\tau^- \to f_1\pi^-\nu_\tau$ decay appears to be a major component of the $\tau^- \to h^-h^+h^-\eta\nu_\tau$ channel. Using the combined measurements for both decays and taking into account the correlations in the $\eta \to \gamma\gamma$ analysis, we find the ratio $\mathcal{B}(\tau^- \to f_1\pi^-\nu_\tau \to \pi^-\pi^+\pi^-\eta\nu_\tau)/\mathcal{B}(\tau^- \to h^-h^+h^-\eta\nu_\tau) = 0.59 \pm 0.17$.

The measured branching fraction of the decay $\tau^- \to \pi^-\pi^+\pi^-\eta\nu_\tau$ is more than two orders of magnitude larger than the value calculated by Pich [4] under the assumption that this decay is dominated by an ηa_1 intermediate state, which is heavily suppressed by phase space. In a very recent calculation, Li [10] using similar assumptions, obtains a branching fraction for $\tau \to f_1\pi\nu_\tau$ which is an order of magnitude smaller than the present measurement.

The decay $\tau \to 3\pi\eta\nu_\tau$ has important implications for the phenomenology of the multipion τ decays, especially for $\tau \to 6\pi\nu_\tau$. Several authors [11-13] have used isospin relations to relate the relative amounts of $\tau \to 5\pi^\pm\pi^\circ\nu_\tau$, $\tau \to 3\pi^\pm 3\pi^\circ\nu_\tau$ and $\tau \to \pi^\pm 5\pi^\circ\nu_\tau$, and have suggested discrepancies with CVC predictions obtained from $e^+e^- \to 6\pi$ measurements. It now appears that $\tau \to 5\pi^\pm\pi^\circ\nu_\tau$ and $\tau \to 3\pi^\pm 3\pi^\circ\nu_\tau$ have large contributions from the $\tau \to \eta 3\pi\nu_\tau$ channel. Since this channel has G parity opposite to that of the direct 6π decays and proceeds through the axial-vector current, it must be subtracted before applying isospin relations or using CVC to compare with e^+e^- annihilation data.

We thank F. Gilman for useful discussions. We gratefully acknowledge the effort of the CESR staff in providing us with excellent luminosity and running conditions. J.P.A., J.R.P., and I.P.J.S. thank the NYI program of the NSF, M.S thanks the PFF program of the NSF, G.E. thanks the Heisenberg Foundation, K.K.G., M.S., H.N.N., T.S., and H.Y. thank the OJI program of DOE, J.R.P, K.H., and M.S. thank the A.P. Sloan Foundation, and A.W., and R.W. thank the Alexander von Humboldt Stiftung for support. This work was supported by the National Science Foundation, the U.S. Department of Energy, and the Natural Sciences and Engineering Research Council of Canada.

REFERENCES

[1] M.Artuso *et al.*, Phys. Rev. Lett. **69**, 3278 (1992).
[2] J. Bartelt *et al.*, Phys. Rev. Lett. **76**, 4119 (1996).
[3] P. Bourdon, Contribution to the Europhysics Conference on High Energy Physics, Brussels, EPS-0242 (1995).
[4] A.Pich, Phys. Lett. **B196**, 561 (1987).
[5] CLEO Collaboration, Y. Kubota *et al.*, Nucl. Instr. Meth. Phys. Res., Sect. A**320**, 66 (1992)
[6] S. Jadach and Z. Was, Comput. Phys. Commun, **36**, 191 (1995).
[7] M. Aguilar-Benitez et al. (PDG), Phys. Rev. **D50**, 1173 (1994).
[8] R. Brun *et al.*, GEANT 3.15, CERN DD/EE/84-1.
[9] Monte Carlo events are generated according to phase space and weighted by the "V-A" factor $(m_\tau^2 - q^2)(M_\tau^2 + 2q^2)$ and additional P-wave barrier factor $\left(\frac{2p_\pi}{\sqrt{q^2}}\right)^3$ where p_π is the momentum of the pion in the $f_1\pi$ center of mass.
[10] Bing An Li, Theory of τ mesonic decays. University of Kansas preprint UK-96-4 (June 1996).
[11] A. Donnachie and A. B. Clegg, Phys. Rev. **D51**, 4979 (1995).
[12] R. Sobie, Z. Phys. C **69**, 99 (1995).
[13] A. Rouge, Z. Phys. C **70**, 65 (1996).